Algorithms and computations in physics (Oxford Lectures 2024)

Werner Krauth*
Laboratoire de Physique, Ecole normale supérieure, Paris (France)
Rudolf Peierls Centre for Theoretical Physics & Wadham College
University of Oxford (UK)

Fifth lecture: 13 February 2024
(version: 11/02/2024)

This is the second of two lectures on classical particle systems. We discuss the entropic depletion interactions and pressure, one of the difficult subjects in physics. We then move on to discussions of more hard-sphere simulation algorithms, some of them traditional, but mostly cutting-edge, red-hot! We end with an introductory analysis of particle systems with more general interactions than hard spheres. What changes with respect to hard spheres, and is it conceivable to treat true long-range interactions?

Contents

5 Particle systems: Physics and algorithms

5.1 Asakura–Oosawa interaction, the fifth force in nature

5.1.1 The random-clothes-pin model

The random-clothes-pin model consists in what the name indicates: N clothes-pins on a washing line, positioned randomly, as fully defined by Alg. 5.1 (`naive-pin`).

*werner.krauth@ens.fr, werner.krauth@physics.ox.ac.uk

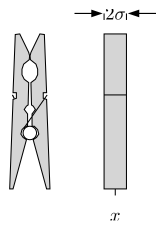

Figure 5.1: A single clothes-pin in side view (*left*) and in front view (*right*).

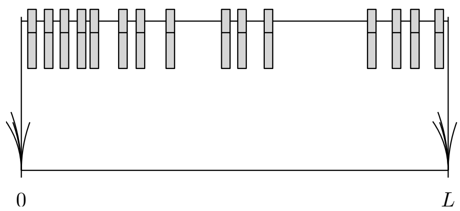

Figure 5.2: $N = 15$ clothes-pins on a washing line of length L.

Attentive participants in these lectures will readily identify this model as a one-dimensional hard-sphere models, again with hard-wall boundary conditions. In addition Alg. 5.1 (`naive-pin`) is but a one-dimensional version of the direct-sampling algorithm for hard disks. We can do much better than Algorithm 5.1 to sample the positions, namely write the direct-sampling method, implemented in Alg. 5.2 (`direct-pin`). It suffices to realize that on a line of length L with N clothes-pins of diameter 2σ, there is $L - 2N\sigma$ of free space. Miraculously, sampling N random numbers `ran`$(0, L - 2N\sigma)$, sorting them, then adding back in the 2σ for the clothes-pins is a correct algorithm, although the `sort` routine, coming out of nowhere, may make us dizzy.

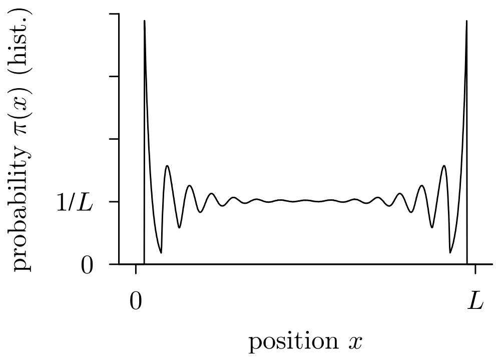

Figure 5.3: Density at position x, obtained by Alg. 5.2 (`direct-pin`).

The above algorithms sample the integral:

$$Z_{N,L} = \int_0^L \cdots \int_0^L \mathrm{d}x_1 \cdots \mathrm{d}x_N \, \pi(x_1, \ldots, x_N), \tag{5.1}$$

where $\pi = 1$ if the configuration is legal and $\pi = 0$ otherwise. The previous transformation from the clothes-pins on a line of length L to points on a line of length $L - 2N\sigma$ shows that the partition function must equal:

$$Z_{N,L} = \begin{cases} (L - 2N\sigma)^N & \text{if } L - 2N\sigma > 0 \\ 0 & \text{else} \end{cases}. \tag{5.2}$$

```
   procedure naive-pin
1  for k = 1, ..., N:
     { x_k ← ran(σ, L − σ)
     { for l = 1, ..., k − 1:
     {   { if |x_k − x_l| < 2σ:  goto 1 (reject sample—tabula rasa)
   output {x_1, ..., x_N}
   ——
```

Algorithm 5.1: `naive-pin`. Direct-sampling algorithm for N pins of width 2σ on a segment of length L (see Alg. **??** (`direct-disks`)).

```
procedure direct-pin
for k = 1, ..., N:
  { ỹ_k ← ran(0, L − 2Nσ)
{y_1, ..., y_N} ← sort[{ỹ_1, ..., ỹ_N}]
for k = 1, ..., N:
  { x_k ← y_k + (2k − 1)σ
output {x_1, ..., x_N}
——
```

Algorithm 5.2: `direct-pin`. Rejection-free direct-sampling algorithm for N pins of width 2σ on a line segment of length L.

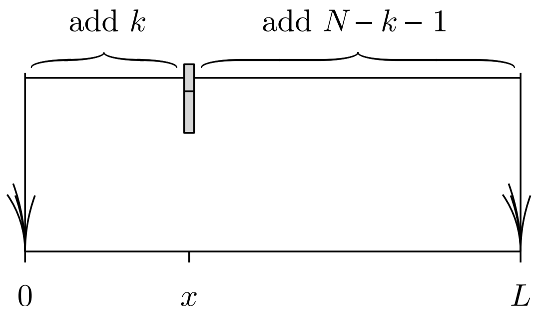

Figure 5.4: Computing the probability of having a clothes-pin at position x.

We may want to check whether the output of Alg. 5.2 (`direct-pin`) is indeed the same as tht of Alg. 5.1 (`naive-pin`). Instead, let us obtain the distribution of Fig. 5.3 analytically. Clearly, the probability $\pi(x)$ is given by the total statistical weight of adding k clothes-pins to the left, and $N-k-1$ clothes-pins to the right of the pin at x (see Fig. 5.4), and this gives:

$$\pi(x) = \sum_{k=0}^{N-1} \underbrace{\frac{1}{Z_{N,L}} \binom{N-1}{k} Z_{k,x-\sigma} Z_{N-1-k,L-x-\sigma}}_{\pi_k(x)} . \tag{5.3}$$

where, fortunately, we defined $zpinNL$ even if one cannot fit N clothes-pins into the space L.

One may plot eq. (5.3), and convince ourselves that it reproduces Fig. 5.3. The walls thus do attract the clothes-pins. The density there is 4 times larger than in the bulk. It is as if the pins had been glued to the post! Asakura and Oosawa, in a famous paper of 1954 [1], understood that the interaction that we see in Fig. **??** is real, and not just a mathematical artifact. To use a drastic statement: replace the clothes-pins by red blood cells, and the two posts by the inner linings of our arteries. The attraction of blood cells to the walls (plus some minor details that we may safely neglect ;)), is what creates heart attacks.

As a first defensive strategy, one might think that the attraction of the clothes-pins with the walls is but a boundary effect. That this is not true can be seen by placing N pins onto a ring with periodic boundary conditions (see Fig. 5.5). We see that the attraction of the pins to the wall is the same as the mutual attraction of neighboring particles. They also attract each other strongly.

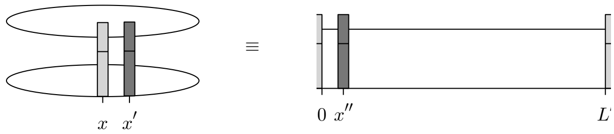

Figure 5.5: Computing the probability of having a clothes-pin at position x.

In conclusion, we have in this section studied the random-clothes-pin model, but have left out one detail, which is Markov-chain Monte Carlo algorithms, which has blossomed into its own little field [2, 3]. Nevertheless, we have understood that there is a curious interaction between particles, even if they have no interaction except that of steric hard spheres. We have come up with a curious direct-sampling algorithm and wonder whether we can generalize it to higher dimensions. The answer will be: "Yes, certainly", but it will not be completely self-evident of how to get there.

5.1.2 Depletion: pictures in one and higher dimensions

The interpretation of the curious interaction between two clothes-pins relies on the concept of a *halo*. A pin, at position x—the center of the pin—does not allow another pin to lie in the interval $[x-\sigma, x+\sigma]$, because of the wooden material of the pin, but in addition two other intervals $[x-2\sigma, x-\sigma]$, and $[x+\sigma, x+2\sigma]$, the halo. Halos are attached to the posts, in addition to the pins, but they behave strangely. For example, two halos can overlap, leaving more space for the others (see [**?**]).

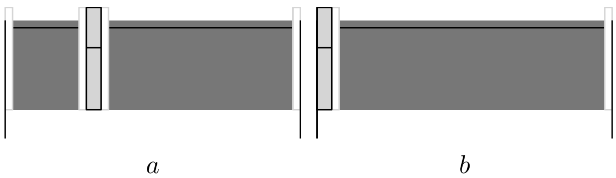

Figure 5.6: Halos at work in the random clothes-pins model for $N = 1$. (a): Halos are attached to the sticks and to the pin, and they do not overlap. (b): Overlapping halos leave more space for the next pin.

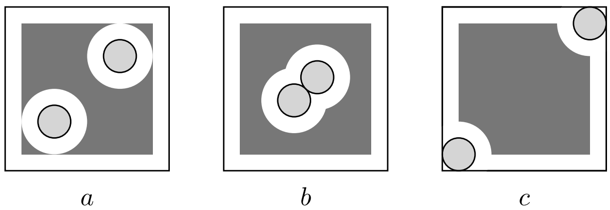

Figure 5.7: Two hard disks, with their halos in a two-dimensional square box

The halo picture is naive as it cannot explain, for example, the wild oscillations of the effective interaction potential, but it is limpid, and it can be easily transposed to higher dimensions (see Fig. 5.7). The interaction that it engenders is called *depletion*, and it may be called the "fifth" force in nature. It describes, as we already discussed, heart attacks, but also super-glues (which are made of polymers, where depletion is the dominant interaction) polymers. Entropic interactions may also extend beyond soft-condensed-matter physics, as some string theorists have argued [4], with concepts of "emergent gravity" potentially mirroring our *emergent* "clothes-pin—post" depletion interaction. [1]

5.1.3 Pressure

Unrelated to the above depletion interaction, we wish to discuss the concept of *pressure*, arguably a most fundamental thermodynamic quantity, but certainly a very tricky one. We can give two representation of the pressure:

1. The (kinetic) pressure is what results, in the system of 4 hard disks in a square box of length 1, from the bangs of the disks in molecular dynamics at the walls, averaged over time and weighted with a factor $2v^{\perp}$, the velocity normal to the wall.

2. The (thermodynamic) pressure is what results from the fundamental relation: In statistical mechanics, the pressure P is given by the change of the free energy with the system volume:

$$\beta P = \frac{\partial \log Z}{\partial V} = \lim_{V' \to V} \frac{1}{V - V'} \frac{Z - Z'}{Z}, \tag{5.4}$$

   with Z the partition function and $Z' \equiv Z(V')$. For hard disks and related models, the rightmost fraction in eq. (5.4) expresses the probability that a sample in the original box of volume V is eliminated in the box of reduced volume $V' < V$ (see Fig. 5.8a-c). In rift-pressure estimators [5], the volume V of an $L_x \times L_y$ box is reduced by removing an infinitesimal vertical or horizontal slab (a "rift"), yielding the components P_x and P_y of the pressure.

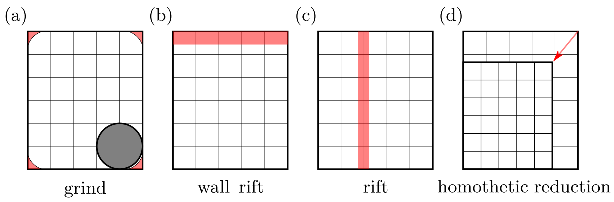

Figure 5.8: Volume changes in a finite box

The wall rift in Fig. 5.8 is not the most efficient estimator for the pressure but it offers an opportunity to check in one dimension, where we can compute, on the one hand, the pressure using eq. (5.4) and, on the other hand, realize that the configurations that disappear with a wall rift are precisely those with a clothes-pin all the way to the right. Their number is directly

[1] I am indebted to the late Prof. Nick Kaiser for discussions on depletion interactions in different fields of physics.

related to the density at the wall, and we computed it! EDMD wall-rift estimator:

$$\beta P_x = \frac{1}{2L_y\tau_{\text{sim}}} \sum_{w:(i,\pm\hat{\mathbf{e}}_x)} \frac{2}{|v^{\perp}_{(i)}|} \tag{5.5a}$$

$$= \left\langle \frac{2}{|v^{\perp}_{\text{wall}}|} \right\rangle \overbrace{\frac{1}{2L_y\tau_{\text{sim}}} \sum_{w:(i,\pm\hat{\mathbf{e}}_x)} 1}^{\hat{n}^{\pm\hat{\mathbf{e}}_x}_{\text{wall}}} \tag{5.5b}$$

$$= \frac{2\sqrt{\pi}}{\sqrt{\sum v_i^2}} \frac{\Gamma(N+\frac{1}{2})}{\Gamma(N)} \hat{n}^{\pm\hat{\mathbf{e}}_x}_{\text{wall}} \tag{5.5c}$$

$$\xrightarrow{N\to\infty} \sqrt{2\pi\beta m}\hat{n}^{\pm\hat{\mathbf{e}}_x}_{\text{wall}}. \tag{5.5d}$$

Here is the kinematic EDMD estimator:

$$P_x = \frac{1}{2L_y\tau_{\text{sim}}} \sum_{w:(i,\pm\hat{\mathbf{e}}_x)} 2m|v^{\perp}_{\text{wall}}| \tag{5.6a}$$

$$= 2m \left\langle |v^{\perp}_{\text{wall}}| \right\rangle \hat{n}^{\pm\hat{\mathbf{e}}_x}_{\text{wall}} \tag{5.6b}$$

$$= \frac{mR_v\sqrt{\pi}}{N} \frac{\Gamma(N+\frac{1}{2})}{\Gamma(N)} \hat{n}^{\pm\hat{\mathbf{e}}_x}_{\text{wall}}, \tag{5.6c}$$

$$\xrightarrow{N\to\infty} \sqrt{2\pi\beta m}\hat{n}^{\pm\hat{\mathbf{e}}_x}_{\text{wall}}, \tag{5.6d}$$

The distribution of the velocity perpendicular to a wall is derived from the surface element on the hypersphere of radius $R_v = \sqrt{v_1^2 + \cdots + v_n^2}$ in $n = 2N$ dimensions:

$$\mathrm{d}\Omega = R_v^{n-1} \sin^{n-2}\phi_1 \sin^{n-3}\phi_2 \ldots \sin\phi_{n-2} \mathrm{d}\phi_1 \ldots \mathrm{d}\phi_{n-1}, \tag{5.7}$$

where $\phi_1, \ldots, \phi_{n-2} \in [0, \pi]$ and $\phi_{n-1} \in [0, 2\pi]$, and where only $v_1 = R_v \cos\phi_1$ is expressed in terms of a single angle. It is thus convenient to identify v_1 with $v^{\perp}_{\text{wall}}$. The radius R_v of the hypersphere at the microcanonical energy $E = mR_v^2/2$ is related to the inverse temperature in the canonical ensemble as $R_v^2 = 2N/(m\beta)$. With the integrals

$$\begin{aligned} A &= \int_0^{\pi} \mathrm{d}\phi_1 |\cos\phi_1| \sin^{n-2}\phi_1 = \frac{2}{n-1}, \\ B &= \int_0^{\pi} \mathrm{d}\phi_1 \sin^{n-2}\phi_1 = \sqrt{\pi}\frac{\Gamma[(n-1)/2]}{\Gamma(n/2)}, \end{aligned} \tag{5.8}$$

this yields:

$$\left\langle \frac{1}{|v^{\perp}_{\text{wall}}|} \right\rangle = \frac{1}{R_v}\frac{B}{A} = \frac{\sqrt{\pi}}{R_v}\frac{\Gamma(N+\frac{1}{2})}{\Gamma(N)} \xrightarrow{N\to\infty} \sqrt{\frac{\pi m\beta}{2}}, \tag{5.9a}$$

$$\left\langle |v^{\perp}_{\text{wall}}| \right\rangle = R_v \frac{B}{2NA} = \frac{R_v\sqrt{\pi}}{2N}\frac{\Gamma(N+\frac{1}{2})}{\Gamma(N)} \xrightarrow{N\to\infty} \sqrt{\frac{\pi}{2m\beta}}, \tag{5.9b}$$

where in the limit $N \to \infty$ the ratio of the Γ functions approaches $\sqrt{N}$.

5.2 More hard-sphere Monte Carlo algorithms

We discuss a number of hard-sphere algorithm, but first consider a single particle.

5.2.1 Coupling from the past

In a previous lecture, we discussed stopping rules (for the card-shuffling applications). We succeeded in fast and perfect sampling from the set of all ordering of a game of cards, using a Markov chain. The domain of perfect sampling was greatly extended, about 25 years ago, through the approach of *coupling from the past*, that we now explain for a single particle.

Consider a single particle moving on a lattice of five sites. Suppose it moves with probability $\frac{1}{3}$ one step down, straight, one step up (see Fig. 5.9).

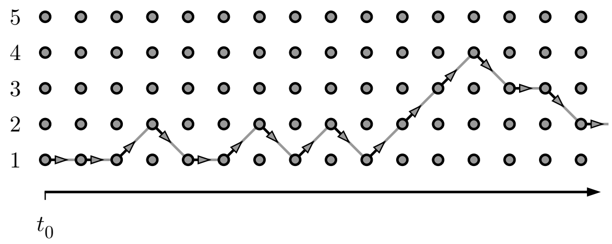

Figure 5.9: Diffusion of a particle on 5 sites.

procedure `forward-coupling`
$\mathcal{P} \leftarrow \{1, \ldots, N\}$
$t \leftarrow 0$
while True:
$\begin{cases} t \leftarrow t + 1 \\ \mathcal{P} \leftarrow \{\min[\max(b + \texttt{choice}(-1, 0, +1), N] \text{ for } b \in \mathcal{P}\} \\ \textbf{if } |\mathcal{P}| = 1\textbf{: break} \end{cases}$
output $\mathcal{P}, t$ (position, time of coupling)
——

Algorithm 5.3: `forward-coupling`. Forward coupling algorithm

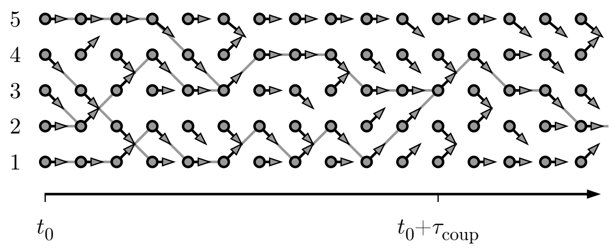

Figure 5.10: Diffusion of a particle on 5 sites using random maps. The position where particles couple is not a sample of π.

5.2.2 Coupling algorithms in higher dimensions

Coupling, a concept introduced in the 1030s by the French–German mathematician W. Doeblin, is not confined to simple test cases. We can also make it work in higher dimensions. We discuss here the algorithm of Mahoney et al., which uses halos in a clever way.

We use that at low density, any two configurations of spheres a and z can be connected through a path of length $< 2N$ as follows: $a \to b \to c \to ..... \to z$, where any two neighbors differ only

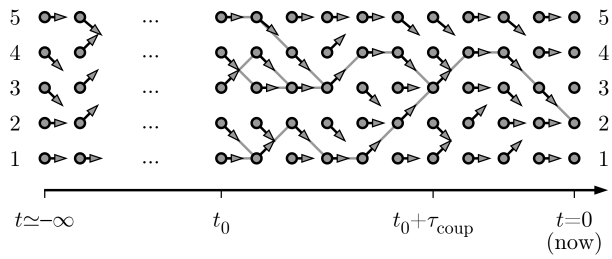

Figure 5.11: Diffusion of a particle on 5 sites using the coupling-from-the-past approach. The position at $t = 0$ is a perfect sample, if we can find it from $t = -\infty$.

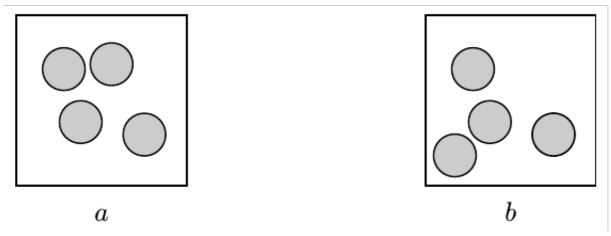

Figure 5.12: Path coupling: At low enough density, any two configurations of N hard disks can be connected through a path of $\sim N$ steps which differ in one disk position only.

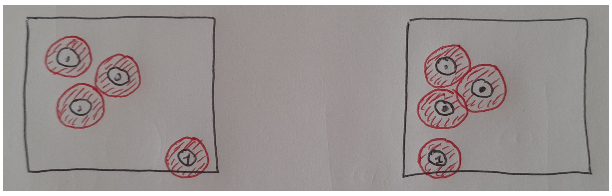

Figure 5.13: text

procedure `coupling-from-past`
$t_{\text{tot}} \leftarrow 0$
while True:
$\left\{ \begin{array}{l} t_{\text{tot}} \leftarrow t_{\text{tot}} - 1 \\ \mathcal{A}_{t_{\text{tot}}} \leftarrow \texttt{draw-arrows} \text{ (draw arrows at time } t_{\text{tot}}) \\ \textbf{for } t = t_{\text{tot}}, t_{\text{tot}} + 1, \ldots, -1\textbf{:} \\ \quad \{ \ \mathcal{P} \leftarrow \{b + \mathcal{A}_t(b) \text{for } b \in \mathcal{P}\} \\ \textbf{if } |\mathcal{P}| = 1\textbf{: break} \end{array} \right.$
output $\mathcal{P}$ (perfect sample)
——

Algorithm 5.4: `coupling-from-past`. Coupling-from-the-past algorithm for diffusion.

in 1 sphere. MC algorithm: Take random sphere, place it at random position anywhere in the box. This is Alg. **??** (`markov-disk`), but with a throwing range which is half of the entire box.

We now couple two configurations MC algorithm: Take random sphere, place it at the same random position for both copies.

- $p(1 \to 0)$: Pick 1, move to where it fits in both copies

$$p(1 \to 0) \geq \frac{1}{N} \left[1 - \frac{N-1}{N} 4\eta \right]$$

- $p(1 \to 2)$: Pick $2 \ldots N$ move near to 1_A or 1_B.

$$p(1 \to 2) \leq \frac{N-1}{N} \left[\frac{8}{N} \eta \right]$$

- $\implies$ for $\eta < 1/12$: further coupling likely.

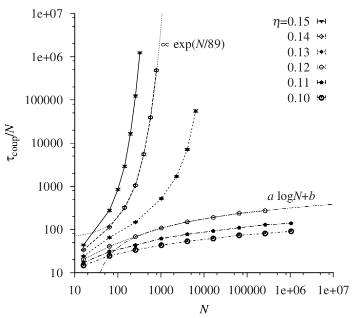

Figure 5.14: text

- Coupling time of PathCoupling algorithm
- NB: $0.12 > 1/12$
- "Physical" relevance of the transition at $\eta = 0.12$?

5.2.3 Non-reversibility

Explain straight event-chain Monte Carlo algorithm, and show that it satisfies the global-balance condition

5.3 Interacting-particle systems

5.3.1 Monte Carlo and molecular dynamics for interacting particles

5.3.2 Long-range interactions with and without cutoffs

5.3.3 Phase transitions in two dimensions

References

[1] S. Asakura and F. Oosawa, "On Interaction between Two Bodies Immersed in a Solution of Macromolecules," *J. Chem. Phys.*, vol. 22, pp. 1255–1256, 1954.

[2] S. C. Kapfer and W. Krauth, "Irreversible Local Markov Chains with Rapid Convergence towards Equilibrium," *Phys. Rev. Lett.*, vol. 119, p. 240603, 2017.

[3] F. H. L. Essler and W. Krauth, "Lifted TASEP: a Bethe ansatz integrable paradigm for non-reversible Markov chains," 2023.

[4] E. P. Verlinde, "Emergent Gravity and the Dark Universe," *SciPost Phys.*, vol. 2, p. 016, 2017.

[5] M. Michel, S. C. Kapfer, and W. Krauth, "Generalized event-chain Monte Carlo: Constructing rejection-free global-balance algorithms from infinitesimal steps," *J. Chem. Phys.*, vol. 140, no. 5, p. 054116, 2014.